Synthesis and Characterization of Donor–Acceptor Poly(3-hexylthiophene) Copolymers Presenting 1,3,4-Oxadiazole Units and Their Application to Photovoltaic Cells

HSU-SHEN WANG, MING-SHIN SU, KUNG-HWA WEI

Department of Materials Science and Engineering, National Chiao Tung University, 300 Hsinchu, Taiwan, Republic of China

Received 8 March 2010; accepted 4 May 2010
DOI: 10.1002/pola.24117
Published online in Wiley InterScience (www.interscience.wiley.com).

ABSTRACT: We have used Grignard metathesis polymerization to prepare poly(3-hexylthiophene)-based copolymers containing electron-withdrawing 4-*tert*-butylphenyl-1,3,4-oxadiazole-phenyl moieties as side chains. We characterized these copolymers using ^{1}H and ^{13}C nuclear magnetic resonance spectroscopy, thermogravimetric analysis, and gel permeation chromatography. The band gap energy of copolymer was determined from the onset of the optical absorption. The quenching effects were observed in the photoluminescence spectra of the copolymers incorporating pendant electron-deficient 1,3,4-oxadiazole moieties on the side chains. The photocurrents of devices were enhanced in the presence of an optimal amount of the 1,3,4-oxadiazole moieties, thereby leading to improved power conversion efficiencies. © 2010 Wiley Periodicals, Inc. J Polym Sci Part A: Polym Chem 48: 3331–3339, 2010

KEYWORDS: conjugated polymers; copolymerization; heteroatom-containing polymers; oxadiazole; photovoltaic cell

INTRODUCTION Conjugated polymers possessing extended delocalized π electrons are being investigated intensively for their potential uses in such organic optoelectronic devices as light-emitting diodes (LEDs), thin film transistors, and photovoltaic cells incorporating bulk heterojunctions.[1–9] Bulk heterojunctions based on blends of poly(3-hexylthiophene) (P3HT) and [6,6]-phenyl-C_{61}-butyric acid methyl ester (PCBM) have recently reached power conversion efficiencies of ~4–5% under standard solar illumination (AM 1.5G, 100 mW cm^{-2}).[10–14] Research into conjugated polymers containing electron donor–acceptor pairs in the polymeric main chain and/or side chains has become quite attractive recently[15–22] because such system exhibits tunable electronic properties and enlarged spectral absorption ranges. Alternatively, the introduction of a side-chain electron-acceptor unit—usually a conjugated species that absorbs a wavelength different from that of the conjugated polymer—can increase the breadth of the wavelengths of light absorbed. Furthermore, the photogenerated excitons can be dissociated into electrons and holes more efficiently in these types of conjugated polymer because of the internal field produced by the inherent dipole moment resulting from the donor–acceptor molecular structure, with subsequent charge transfer to nearby *n*-type nanoparticles (e.g., PCBM). In previous studies, we developed a new class of conjugated polymers containing side chain–tethered conjugated acceptor moieties that not only absorb light more effectively but also exhibit enhanced charge transfer ability—two desirable properties for photovoltaics applications.[23–25]

Most polythiophene derivatives are good hole-transport materials but exhibit low electron mobility. Oxadiazole-containing polymers have been widely applied as electron-transporting and hole-blocking materials in organic electronic devices[26–29] (e.g., organic LEDs) because of the strong electron-withdrawing ability of the heterocycle, their good thermal and chemical properties,[30–32] and the tenability of the charge carrier mobility of attached materials.[33,34] Oxadiazole units have previously been incorporated as side chains on poly(phenylenevinylene) (PPV) and polyfluorene (PF) derivatives that have then been incorporated into photovoltaic cells without PCBM.[35] The performance of these devices was improved as a result of increases in the electron mobility and rate of exciton dissociation in the photoactive layer. Furthermore, PPV derivatives featuring branched oxadiazole units within the PPV main chain have been applied as a PCBM blend to provide a photovoltaic cell exhibiting a PCE of 1.6%.[36] In contrast, the photovoltaic behavior of oxadiazole-attached polythiophene copolymers has not been reported previously.

In this study, we synthesized a donor–acceptor thiophene-type copolymer presenting electron-withdrawing 1,3,4-oxadiazole moieties as side chains for application in photovoltaic cells. Schemes 1 and 2 display our synthetic approach

Additional Supporting Information may be found in the online version of this article. Correspondence to: K.-H. Wei (E-mail: khwei@mail.nctu.edu.tw)
Journal of Polymer Science: Part A: Polymer Chemistry, Vol. 48, 3331–3339 (2010) © 2010 Wiley Periodicals, Inc.

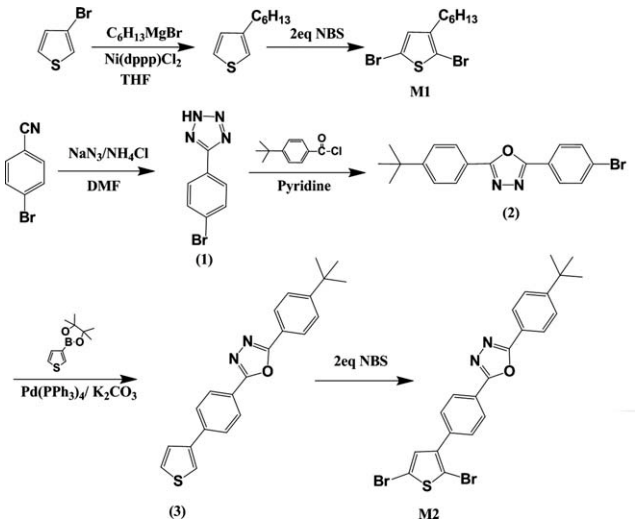

SCHEME 1 Synthetic routes toward **M1** and **M2**.

toward a thiophene monomer modified with an electron-withdrawing moiety and its subsequent polymerization.

EXPERIMENTAL

Materials

2,5-Dibromo-3-hexylthiophene (**M1**) and 4,4,5,5-tetramethyl-2-(thiophen-3-yl)-1,3,2-dioxaborolane were synthesized according to literature procedures.[37–41] The synthetic routes toward monomer **2** (**M2**) and polymers **P05–P20** are presented in Schemes 1 and 2; procedures for the syntheses of their intermediates are described below. The 3 M ether solution of methylmagnesium bromide was purchased from TCI. PCBM was purchased from Nano-C. Regioregular P3HT was purchased from Rieke Metals (4002-E). Poly(ethylenedioxythiophene)/poly(styrenesulfonate) (PEDOT/PSS) was purchased from Baytron (P VP A1 4083). All other chemicals and solvents were purchased in reagent grade from Aldrich, Acros, TCI, or Lancaster Chemical and used as received.

Measurement and Characterization

^1H and ^{13}C nuclear magnetic resonance (NMR) spectra were recorded using a Varian Unity-300 NMR spectrometer. Thermogravimetric analysis (TGA) of the polythiophene derivatives was performed using a TA Instruments Q500 apparatus operated at a heating rate of 20 °C min^{-1} under a N_2 flow. Differential scanning calorimetry (DSC) was performed using a Perkin–Elmer Pyris 7 instrument operated at a heating rate of 20 °C min^{-1} under N_2 flow; samples were heated from 30 to 200 °C, cooled to 20 °C, and then heated again from 30 to 200 °C. Elemental analysis (EA) of the polymers was performed using a Heraeus CHN-OS Rapid instrument. UV–vis spectra were measured using an HP 8453 diode array spectrophotometer. PL spectra were recorded using a Hitachi F-4500 luminescence spectrometer. We used a Waters chromatography unit interfaced to a Waters 2414 differential refractometer. Three 5-μm Waters styragel columns were connected in series in decreasing order of pore size (10^4, 10^3, and 10^2 Å); THF was the eluent and standard polystyrene samples were used for calibration. Cyclic voltammetry (CV) was performed using a BAS 100 electrochemical analyzer, operated at a potential scan rate of 50 mV s^{-1}; the redox behavior of each polymer was investigated using a solution of 0.1 M tetrabutylammonium hexafluorophosphate in anhydrous acetonitrile as the electrolyte; the potentials were measured against a Ag/Ag^+ (0.01 M $AgNO_3$) reference electrode; ferrocene/ferrocenium ion (Fc/Fc^+) was used as the internal standard. The onset potentials were determined from the intersection of two tangents drawn at the rising and background currents of the cyclic voltammogram. The topographies of the polymer/PCBM films were measured through tapping-mode atomic force microscopy (AFM) using a Digital Instruments Nanoscope IIIa apparatus under ambient conditions; AFM samples were prepared by spin-coating solutions of polymer/PCBM blends in chlorobenzene onto indium tin oxide (ITO)/PEDOT substrates, followed by annealing at 150 °C for 10 min.

Device Fabrication and Characterization of Polymer Solar Cell

Current density–voltage (*J–V*) measurements were performed using devices having a sandwich structure [ITO/PEDOT:PSS/polymer:PCBM (1:1, w/w)/Ca/Al]. The ITO-coated glass substrate was precleaned and treated with oxygen plasma before use. The polymer/PCBM layers were spin-coated from their corresponding dichlorobenzene solutions (20 mg mL^{-1}) at 1500 rpm. The thickness of the polymer/PCBM layers was ~100 nm. The active layers of the devices were thermally annealed at 150 °C for 10 min before electrode deposition. Using a base pressure of $<1 \times 10^{-6}$ Torr, layers of Ca (20 nm) and Al (100 nm) were vacuum-deposited to form the anode. The effective area of one cell was 0.04 cm^2.

The devices were tested under simulated AM 1.5G irradiation (100 mW cm^{-2}) using a Xe lamp-based Newport 66902 150-W solar simulator equipped with an AM1.5 filter as the white light source; the optical power at the sample was 100 mW cm^{-2}, detected using an OPHIR thermopile 71964. The *J–V* characteristics were measured using a Keithley 236 source-measure unit. The external quantum efficiencies (EQEs) were measured using a Keithley 236 source-measure unit coupled with an Oriel Cornerstone 130 monochromator. The light intensity at each wavelength was calibrated using an OPHIR 71580 diode.

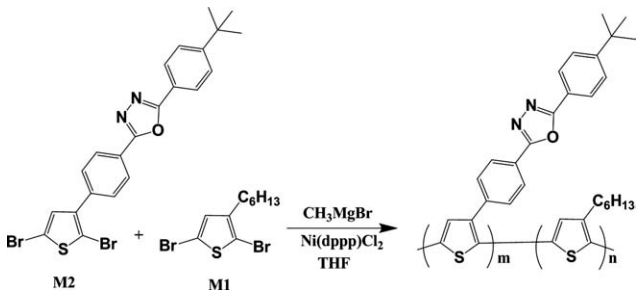

SCHEME 2 Synthetic route toward the copolymers.

5-(4-Bromophenyl)-2*H*-tetrazole (1)

A mixture of 4-bromobenzonitrile (5.00 g, 27.6 mmol), sodium azide (5.35 g, 82.3 mmol), NH_4Cl (4.40 g, 82.2 mmol), and DMF (15 mL) was heated for 4 h under N_2 in an oil bath maintained at a bath temperature of 150 °C. After cooling to room temperature, the solution was poured into 1 N HCl (150 mL) and stirred for 30 min. After filtering, the solid product was washed with water (3 × 300 mL) and dried to yield **1** (5.30 g, 85%).

^{1}H NMR (300 MHz, DMSO-d_6, ppm): 7.20 (d, J = 8.7 Hz, 2H), 7.04 (d, J = 8.7 Hz, 2H). ^{13}C NMR (75 MHz, DMSO-d_6, ppm): 155.9, 133.2, 129.6, 125.6, 123.9. HRMS-EI (m/z): [M^+] Calcd. for $C_7H_5BrN_4$, 223.9698; Found, 223.9692.

2-(4-Bromophenyl)-5-(4-*tert*-butylphenyl)-1,3,4-oxadiazole (2)

4-*tert*-Butylbenzoyl chloride (3.25 g, 16.5 mmol) was added dropwise to a solution of **1** (2.50 g, 11.1 mmol) in pyridine (30 mL) and then the mixture was heated for 6 h under N_2 in an oil bath maintained at 130 °C. After cooling to room temperature, the solution was poured into water (300 mL). The solid product was filtered off, washed with water (5 × 300 mL), and dried to yield **2** (3.25 g, 82%).

^{1}H NMR (300 MHz, $CDCl_3$, ppm): 8.04 (d, J = 8.7 Hz, 2H), 7.99 (d, J = 8.4 Hz, 2H), 7.66 (d, J = 8.7 Hz, 2H), 7.54 (d, J = 8.4, 2H), 1.34 (s, 9H). ^{13}C NMR (75 MHz, $CDCl_3$, ppm): 164.2, 163.2, 155.1, 132.5, 128.6, 126.6, 126.3, 125.6, 122.6, 120.5, 34.9, 30.8. HRMS-EI (m/z): [M^+] Calcd. for $C_{18}H_{17}BrN_2O$, 356.0524; Found, 356.0527.

2-(4-tert-Butylphenyl)-5-[4-(thiophen-3-yl)phenyl]-1,3,4-oxadiazole (3)

A total of 2 M aqueous potassium carbonate (11 mL) was added via syringe to a solution of **2** (3.00 g, 8.40 mmol), 4,4,5,5-tetramethyl-2-(thiophen-3-yl)-1,3,2-dioxaborolane (1.80 g, 8.53 mmol), and tetrakis(triphenylphosphine)palladium (2 mol %) in toluene (22 mL) in a 50-mL two-neck flask. The mixture was then stirred overnight at 90 °C under N_2. After cooling to room temperature, the solution was washed with water and back-extracted with EtOAc. The organic layer was dried ($MgSO_4$) and concentrated to yield **3** (2.70 g, 90%).

^{1}H NMR (300 MHz, $CDCl_3$, ppm): 8.17 (d, J = 8.1 Hz, 2H), 8.08 (d, J = 8.1 Hz, 2H), 7.77 (d, J = 8.1 Hz, 2H), 7.61–7.59 (m, 1H), 7.56 (d, J = 8.4 Hz, 2H), 7.48–7.43 (m, 2H), 1.38 (s, 9H). ^{13}C NMR (75 MHz, $CDCl_3$, ppm): 164.6, 164.2, 155.3, 141.0, 138.8, 127.4, 126.8, 126.7, 126.2, 126.0, 124.3, 122.5, 121.7, 121.1, 35.1, 31.1. HRMS-EI (m/z): [M^+] Calcd. for $C_{22}H_{20}N_2OS$, 360.1296; Found, 360.1287.

2-(4-tert-Butylphenyl)-5-[4-(2,5-dibromothiophen-3-yl)phenyl]-1,3,4-oxadiazole (M2)

N-Bromosuccinimide (NBS, 2.00 g, 11.2 mmol) was added portionwise to a solution of **3** (2.00 g, 5.55 mmol) in THF (20 mL) and acetic acid (20 mL) and then the mixture was stirred and heated at 80 °C for 6 h. After cooling to room temperature, the solution was washed sequentially with water (2 × 200 mL), saturated $NaHCO_3$ (1 × 200 mL), and then water again (1 × 200 mL). After extraction with EtOAc, the organic layer was dried ($MgSO_4$) and concentrated to yield the monomer **M2** (2.64 g, 92%).

^{1}H NMR (300 MHz, $CDCl_3$, ppm): 8.18 (d, J = 8.7 Hz, 2H), 8.06 (d, J = 8.7 Hz, 2H), 7.67 (d, J = 8.4 Hz, 2H), 7.55 (d, J = 8.4 Hz, 2H), 7.07 (s, 1H), 1.37 (s, 9H). ^{13}C NMR (75 MHz, $CDCl_3$, ppm): 164.8, 163.9, 155.4, 140.8, 137.1, 131.3, 129.1, 127.0, 126.8, 126.0, 123.5, 121.0, 111.8, 108.7, 35.1, 31.1. HRMS-EI (m/z): [M^+] Calcd. for $C_{22}H_{18}Br_2N_2OS$, 517.9507; Found, 517.9457.

Preparation of Polythiophene Derivatives

All polymers were synthesized through Grignard metathesis polymerization in THF according to procedures similar to those described in the literature.[37–39] The Grignard metathesis polymerizations of **M1** and **M2** are presented in Scheme 2.

Poly(3-hexylthiophene)

CH_3MgBr (1.50 mL, 4.50 mmol) was added via syringe to a stirred solution of 2,5-dibromo-3-hexylthiophene (1.60 g, 4.50 mmol) in freshly distilled THF (80 mL) in a three-neck 100-mL round-bottom flask. The solution was heated under reflux for 2 h and then Ni(dppp)Cl_2 (12 mg, 0.02 mmol) was added. The mixture was stirred at 95 °C for 2.5 h before the reaction was quenched through the addition of MeOH. The solid polymer was washed with MeOH and hexane within a Soxhlet extractor; it was then dissolved through Soxhlet extraction with $CHCl_3$, the solvent was evaporated, and the residue dried under vacuum to yield P3HT (0.51 g, 61%). The weight-average molecular weights (M_w) and polydispersity index (PDI) are 15.9 kg mol^{-1}and 1.26, respectively.

^{1}H NMR (300 MHz, $CDCl_3$, ppm): 6.96 (s, 1H), 2.79 (t, 2H); 0.89–0.81, 1.43–1.15, and 1.72–1.45 (m, 11H). ^{13}C NMR (75 MHz, $CDCl_3$, ppm): 139.8, 133.7, 130.4, 128.5, 31.9, 30.6, 29.6, 29.4, 22.7, 14.2. Anal. Calcd: C, 72.23; H, 8.49. Found: C, 72.10; H, 8.30.

P05

CH_3MgBr (0.820 mL, 2.46 mmol) was added via syringe to a stirred solution of 2,5-dibromo-3-hexylthiophene (760 mg, 2.33 mmol), **M2** (63.5 mg, 0.122 mmol), and freshly distilled THF (40 mL) in a three-neck 100-mL round-bottom flask. The solution was heated under reflux for 2 h and then Ni(dppp)Cl_2 (6 mg, 0.01 mmol) was added. The mixture was stirred at 95 °C for 2.5 h and then the reaction was quenched through the addition of MeOH. The solid polymer was washed with MeOH and hexane within a Soxhlet extractor; it was then dissolved through Soxhlet extraction with $CHCl_3$, the solvent was evaporated, and the residue dried under vacuum to yield **P05** (202 mg, 46%). The M_w and PDI are 25.7 kg mol^{-1}and 1.36, respectively.

^{1}H NMR (300 MHz, $CDCl_3$, ppm): 8.3–7.9 (br, 0.25H), 7.7–7.4 (m, 0.25H), 6.96 (s, 1.09H), 2.78 (br, 2.12H), 1.66–1.36 (m, 7.31H), 0.88 (s, 2.98H). ^{13}C NMR (75 MHz, $CDCl_3$, ppm): 140.1, 133.9, 130.7, 129.3, 128.8, 128.5, 127.3, 127.0, 126.3, 31.9, 31.4, 30.7, 29.7, 29.5, 22.9, 14.4. Anal. Calcd: C, 72.30; H, 8.32; N, 0.39. Found: C, 70.15; H, 7.83; N, 0.39.

TABLE 1 Polymerization Data and Thermal Properties of the Copolymers

Polymer	Feed Ratio *m*:*n*	Actual Ratio[a]	Yield (%)	M_n (10^3)	M_w (10^3)	PDI	DSC (T_g, °C)	TGA (T_d, °C)
P3HT	0:*n*	0:*n*	68	12.6	15.9	1.26	55.8	381.2
P05	0.5:9.5	0.5:9.5	65	18.9	25.7	1.36	86.9	364.7
P15	1.5:8.5	1.6:8.4	56	14.5	19.6	1.36	91.8	360.4
P20	2:8	2.6:7.4	62	11.2	13.8	1.24	92.1	355.9

[a] Measured by elemental analysis.

P15

A mixture of CH_3MgBr (0.820 mL, 2.46 mmol), **M1** (680 mg, 2.08 mmol), and **M2** (191 mg, 0.368 mmol) in THF (40 mL) was copolymerized using the method described for the preparation of **P05** to give **P15** (215 mg, 44%). The M_w and PDI are 19.6 kg $mol^{-1}$and 1.36, respectively.

^1H NMR (300 MHz, $CDCl_3$, ppm): 8.3–7.9 (br, 0.64H), 7.7–7.4 (m, 0.65H), 6.96 (s, 1.08H), 2.78 (t, 1.75H), 1.66–1.36 (m, 7.38H), 0.89 (s, 3.1H). ^{13}C NMR (75 MHz, $CDCl_3$, ppm): 140.1, 133.9, 130.7, 129.3, 128.8, 128.5, 127.0, 126.3, 125.5, 31.9, 31.4, 30.7, 29.7, 29.5, 22.9, 14.4. Anal. Calcd: C, 72.45; H, 7.98; N, 1.17. Found: C, 69.91; H, 7.72; N, 1.24.

P20

A mixture of CH_3MgBr (0.820 mL, 2.46 mmol), **M1** (640 mg, 1.96 mmol), and **M2** (254 mg, 0.488 mmol) in THF (40 mL) was copolymerized using the method described for the preparation of **P05** to give **P15** (218 mg, 43%). The M_w and PDI are 13.8 kg mol^{-1} and 1.24, respectively.

^1H NMR (300 MHz, $CDCl_3$, ppm): 8.3–7.9 (br, 0.66H), 7.7–7.4 (m, 0.72H), 6.96 (s, 0.75H), 2.78 (br, 1.33H), 1.66–1.36 (m, 9.7H), 0.89 (s, 1.83H). ^{13}C NMR (75 MHz, $CDCl_3$, ppm): 140.1, 133.9, 130.7, 129.3, 128.8, 128.5, 127.0, 126.3, 125.5, 31.9, 31.4, 30.7, 29.7, 29.5, 22.9, 14.4. Anal. Calcd: C, 72.53; H, 7.80; N, 1.56. Found: C, 70.33; H, 7.70; N, 2.03.

RESULTS AND DISCUSSION

Schemes 1 and 2 illustrate the synthetic routes that we followed for the preparation of the monomers and copolymers. Starting from 4-bromobenzonitrile, Compounds **1** and **2** were prepared via tetrazole routes with relative high yields and simple workup procedures.[42] The Suzuki coupling of Compound **2** with 4,4,5,5-tetramethyl-2-(thiophen-3-yl)-1,3,2-dioxaborolane furnished the desired Compound **3**, which we then brominated with NBS to generate the monomer **M2**. As indicated in Scheme 2, the copolymers were obtained through Grignard metathesis polymerization using various monomer **M1**/**M2** mixtures. The resulting copolymers **P05–P20** are soluble in common organic solvents, including toluene, THF, $CHCl_3$, and chlorobenzene. We characterized the synthesized monomers and copolymers using ^1H and ^{13}C NMR spectroscopy and mass spectrometry.

In the ^1H NMR spectrum of **P15**, the peak at 6.96 ppm (CH proton of the thiophene ring) is absent, whereas broad peaks at 7.9–8.3, 7.4–7.6 (CH protons on the phenyl group), and 0.8–3.0 (hexyl chain and *tert*-butyl group protons) ppm confirm that the copolymer of **M1** and **M2** had formed. We confirmed that the copolymers and the self-made P3HT possessed head-to-tail (regioregular) configurations because the signal at 6.96 ppm was present in the spectra without any other peaks nearby.[33,34] Table 1 displays the actual ratio of polymers, molecular weights, degradation temperatures, and glass transition temperatures of all of our synthesized copolymers. The actual content of oxadiazole pendant side chain groups for P05, P15, and P20 as estimated from EA is 5, 16, and 26 mol %, respectively. The number molecular weights (M_n) of our polymers ranged from 11.2 to 18.9 kg mol^{-1}, with PDIs ranging from 1.24 to 1.36. Each copolymer exhibited outstanding thermal stability, with 5% weight losses temperatures (T_d) greater than 350 °C under N_2 atmosphere. The glass transition temperatures (T_g) increased from 55.8 °C for the self-made P3HT to 92.1 °C for **P20**, because of the stronger interchain interactions among the copolymers.

Optical Properties

Figure 1(a) displays UV–vis spectra of the polymers in THF solution (9.6×10^{-5} M). The small peak at 304 nm was caused by the presence of conjugated 1,3,4-oxadiazole moieties that were not fully coplanar with the polythiophene chain, owing to steric hindrance. The dihedral angle between the plane of oxadiazole moiety and that of thiophene is 32.11° as determined by molecular modeling (ChemBio3D, see Supporting Information Fig. S2.). The absorption maximum wavelength of comonomer (Compound **3**) is 314 nm, which is closed to the absorption of 1,3,4-oxadiazole moieties in copolymer. The π–π^* transitions were responsible for the maximum absorptions (λ_{max}) occurring at ~445 nm for P3HT and at 446 nm for **P15**. Figure 1(b) displays UV–vis spectra of the polymers in the solid state with film thickness 90 nm on quartz. For P3HT, the peak of the π–π^* transition had red-shifted from 445 nm in solution to 521 nm in the solid state; for **P15**, the red-shift was from 446 to 518 nm. These data indicate that efficient π stacking and intermolecular interactions occurred in the films. The vibronic absorption shoulders in the P3HT and **P05–P20** film are a manifestation of high degree of π–π stacking of thiophene planes. Introducing the 1,3,4-oxadiazole moieties to the polymer side chain, however, weakens this π–π stacking and therefore the vibronic shoulders, causing **P15** to have less red-shifted shoulders than that of P3HT. The optical band gaps (E_g^{opt}) of P3HT and **P05–P20**, estimated from the onsets of the absorptions in their solid films, are quite close to one another, in the range 1.89–1.91 eV as shown in the Table 2.

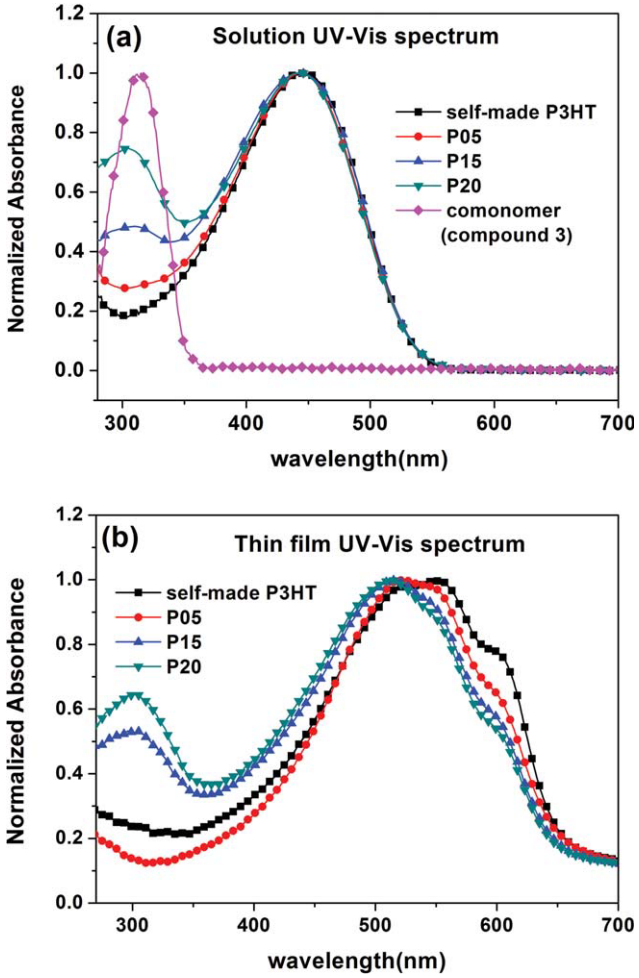

FIGURE 1 Normalized optical absorption spectra of the self-made P3HT, the copolymers **P05–P20**, and comonomer (Compound **3**) in (a) THF solution (9.6×10^{-5} M) and (b) self-made P3HT and the copolymers **P05–P20** as thin films (the thickness of film is 90 nm on quartz). [Color figure can be viewed in the online issue, which is available at www.interscience.wiley.com.]

Figure 2 displays photoluminescence (PL) spectra of polymer films for self-made P3HT and copolymer **P05–P20**. The thickness of film is 90 nm on ITO substrate. The PL spectra are recorded at an excitation wavelength of 450 nm and quenched relative to that of pure P3HT, with the degree of quenching increasing upon increasing the content of 1,3,4-oxadiazole units in the copolymer.

Electrochemical Properties

We used CV to investigate the redox properties of the copolymers and, thereby, estimate the energy levels of their highest occupied molecular orbitals (HOMOs) and lowest unoccupied molecular orbitals (LUMOs). Figure 3 displays the electrochemical behavior of the copolymers in solid films; Table 2 summarizes the relevant data. The 1,3,4-oxadiazole-containing copolymers **P05–P20** exhibited reversible reductions; their onset potentials (~1.74–1.76 V) were slightly lower than that of the self-made P3HT (1.80 V). The CV traces of **P05–P20** feature reversible oxidations; we assign the onset potentials at 0.34–0.38 V (i.e., very close to 0.37 V) to oxidation of the self-made P3HT. From the onset potentials of the copolymers, we estimated HOMO energy levels of the self-made P3HT and **P05–P20** to be 5.17, 5.18, 5.17, and 5.14 eV, respectively, with LUMO energy levels of 3.00, 3.05, 3.04, and 3.06 eV, respectively, according to the energy level of the ferrocene reference (4.8 eV below vacuum level)[43]; the electrochemical band gaps of the self-made **P3HT** and **P05–P20** were 2.17, 2.13, 2.13, and 2.08 eV, respectively. For the copolymers **P05–P20**, the introduction of electron-withdrawing groups on the side chains resulted in slightly lower LUMO energy levels and lower electrochemical band gaps relative to those of the self-made P3HT.

Photovoltaic Properties

Figure 4 displays the photocurrents of diodes having the structure ITO/PEDOT:PSS/polymer:PCBM (1:1, w/w)/Ca/Al that we illuminated under AM 1.5 G conditions (100 mW cm^{-2}), as well as the dark currents measured for self-made P3HT/PCBM and **P15**/PCBM blends. The short-circuit current density (J_{sc}) increased upon increasing the content of 1,3,4-oxadiazole moieties, presumably because of enhanced light absorption at lower wavelengths. Table 3 lists the short-circuit current densities, open-circuit voltages, and PCEs of the heterojunction polymer photovoltaic cells.

The devices based on the self-made P3HT/PCBM and **P05-P15**/PCBM exhibited open-circuit voltages (V_{oc}) of 0.59–0.65 V. Although these values are related to the difference between the HOMO energy level of the copolymers and the LUMO energy level of PCBM,[44] they are also influenced by many other factors, including solvent effects and the miscibility of copolymer and PCBM.

The short-circuit current density (J_{sc}) of the device containing the copolymer featuring 15 mol % 1,3,4-oxadiazole units (**P15**) and PCBM was 8.80 mA cm^{-2}, an improvement of

TABLE 2 Optical and Redox Properties of the Copolymers

Polymer	λ_{max} (nm), Solution	λ_{max} (nm), Film	E_g^{opt} (eV)[a]	E_{ox} (V)	E_{red} (V)	HOMO (eV)[b]	LUMO (eV)[b]
Self-made P3HT	445	521 (553,605)	1.91	0.37	1.80	5.17	3.00
P05	446	521 (546,601)	1.91	0.38	1.75	5.18	3.05
P15	446	518 (545,600)	1.90	0.37	1.76	5.17	3.04
P20	446	517 (545,600)	1.89	0.34	1.74	5.14	3.06

[a] Estimated from the onset wavelength absorptions of the solid films. [b] Calculated from the corresponding onset potentials.

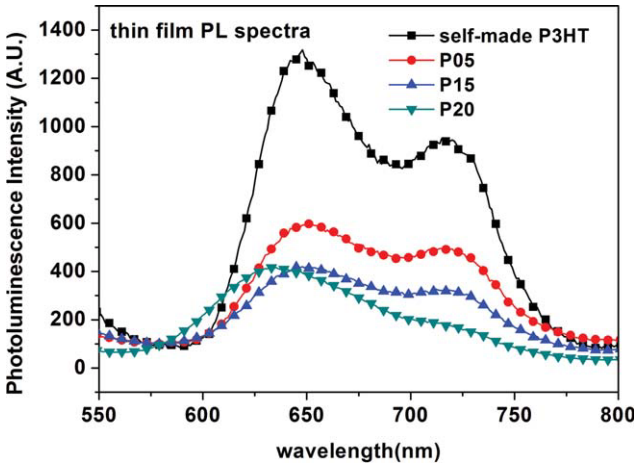

FIGURE 2 PL spectra of films of the self-made P3HT and the copolymers **P05**, **P15**, and **P20**, recorded at an excitation wavelength of 450 nm. The thickness of film is 90 nm on ITO substrate. [Color figure can be viewed in the online issue, which is available at www.interscience.wiley.com.]

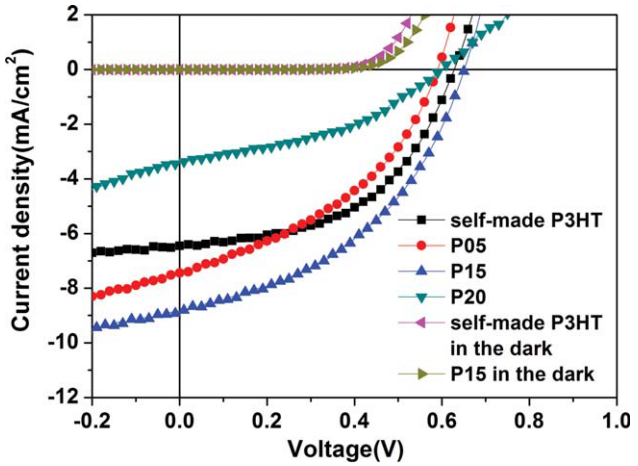

FIGURE 4 Current density–voltage characteristics of illuminated (AM 1.5G, 100 mW cm^{-2}) polymer photovoltaic cells incorporating PCBM blends of the self-made P3HT and the copolymers **P05, P15**, and **P20**. [Color figure can be viewed in the online issue, which is available at www.interscience.wiley.com.]

36% from the value of 6.45 mA cm^{-2} measured for the device containing self-made P3HT. The PCE of the device prepared from the self-made P3HT and PCBM was 2.05%, in agreement with the values reported in the literature.[45] Although the PCE of a device that was prepared using commercially available high-molecular-weight P3HT (M_n = 33,000, 198 repeating units) and PCBM was much higher, that is, 3.40% under the same processing condition as shown in Table 3, we are comparing the effect of different molecular structures on their photovoltaic devices performance at the same effective polymer chain length—the average number of repeating units in the polythiophene-oxadiazole

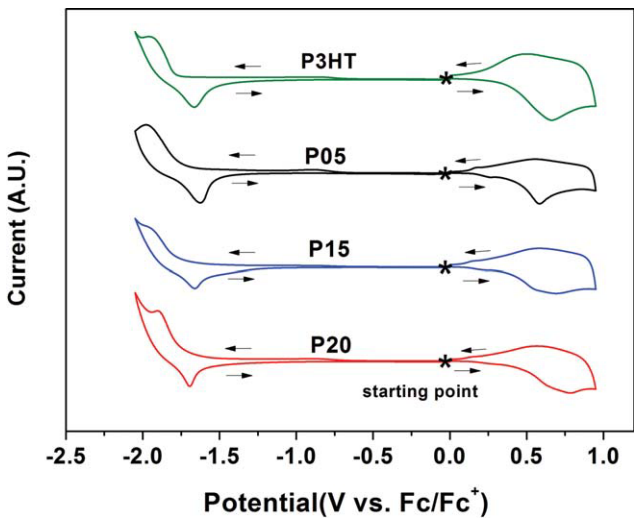

FIGURE 3 Cyclic voltammograms of films of the self-made P3HT and the copolymers **P05**, **P15**, and **P20**, recorded at a scan rate of 50 mV s^{-1}. [Color figure can be viewed in the online issue, which is available at www.interscience.wiley.com.]

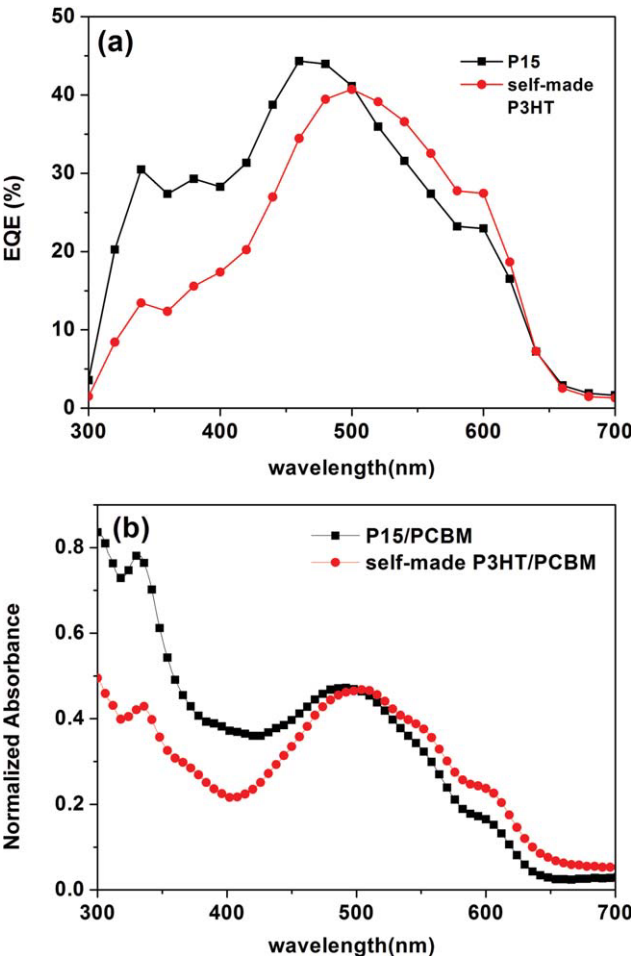

FIGURE 5 (a) EQEs of solar cells incorporating copolymer **P15**/PCBM and the self-made P3HT/PCBM blends. (b) Absorption spectra of the copolymer **P15**/PCBM and the self-made P3HT/PCBM at blend ratios of 1:1. [Color figure can be viewed in the online issue, which is available at www.interscience.wiley.com.]

TABLE 3 Photovoltaic Properties of Polymer Photovoltaic Cells Incorporating Blends (1:1, w/w) of P3HT/PCBM and **P05–P20**/PCBM

Polymer	J_{sc}[a] (mA cm^{-2})	V_{oc}[b] (V)	FF[c] (%)	η[d] (%)
Self-made P3HT (M_n = 12,600)	6.45	0.63	50.0	2.05
P05	7.40	0.59	40.7	1.79
P15	8.80	0.65	43.8	2.50
P20	3.39	0.60	40.8	0.83
Commercial P3HT (M_n = 33,000)	9.79	0.59	59.2	3.42

[a] Short-circuit current density.
[b] Open-circuit voltage.
[c] Fill factor.
[d] Power conversion efficiency.

copolymer **P15** (M_n = 14,500) and the self-made P3HT (M_n = 12,600) were 75 and 76, respectively. Nevertheless, the PCE of the **P15**/PCBM device was 2.50%, 22% higher than the PCE of 2.05% of the device featuring P3HT/PCBM as the active layer. The shape of the EQE curve of the **P15**/PCBM device in Figure 5(a) resembles the shape of the absorption spectrum of the active layer in Figure 5(b), suggesting that the absorbed photons contributed to the induced photocurrent. The EQEs of **P15**/PCBM were at least 10% higher than those of the self-made P3HT/PCBM at wavelengths in the range 320–460 nm. Although the oxadiazole side chains provide the absorption at short wavelength region (around 304 nm), they also weaken the degree of π–π stacking of thiophene planes, resulting in weaker vibronic absorption shoulders. Therefore, the content of oxadiazole side chains should be optimized to provide an additional absorption region and to possess suitable degree of polymer chain ordering for better device performance. The copolymer **P05** only has a small absorption at 304 nm but with decreased chain ordering, see Figure S4 in the Supporting Information. The copolymer **P20** provides much larger absorption at 304 nm, but the excess oxadiazole moieties decreased chain ordering more intensively. Therefore, the device by copolymer **P15** shows the optimal performance. Figure S4 shows the synchrotron grazing-incidence X-ray diffraction patterns of self-made P3HT and **P05–P15**.

Figure 6 displays the surface morphologies determined from AFM measurements. Samples of the self-made P3HT and the copolymer **P05–P20**/PCBM (1:1 w/w) blended films were spin-coated from their corresponding chlorobenzene solutions and then annealed at 150 °C for 10 min, that is, conditions identical to the procedure used to fabricate the active layers of the devices. The root-mean-square (RMS) roughness of the self-made P3HT and **P05–P20** blends was 1.33, 1.531, 0.88, and 1.44 nm, respectively. The larger RMS value for the **P20**/PCBM film suggests its significantly large phase separation. This suitable phase separation and surface roughness facilitated the improved charge transport and carrier collection efficiency, resulting in reduced charge recombination and an increased short-circuit current density. From the AFM images, we assume that the homogeneous morphology of **P15** may have had a significant influence on the device performance.

CONCLUSIONS

We have used Grignard metathesis polymerization to prepare a series of thiophene-based copolymers through conjugation with electron-withdrawing 1,3,4-oxadiazole moieties in the

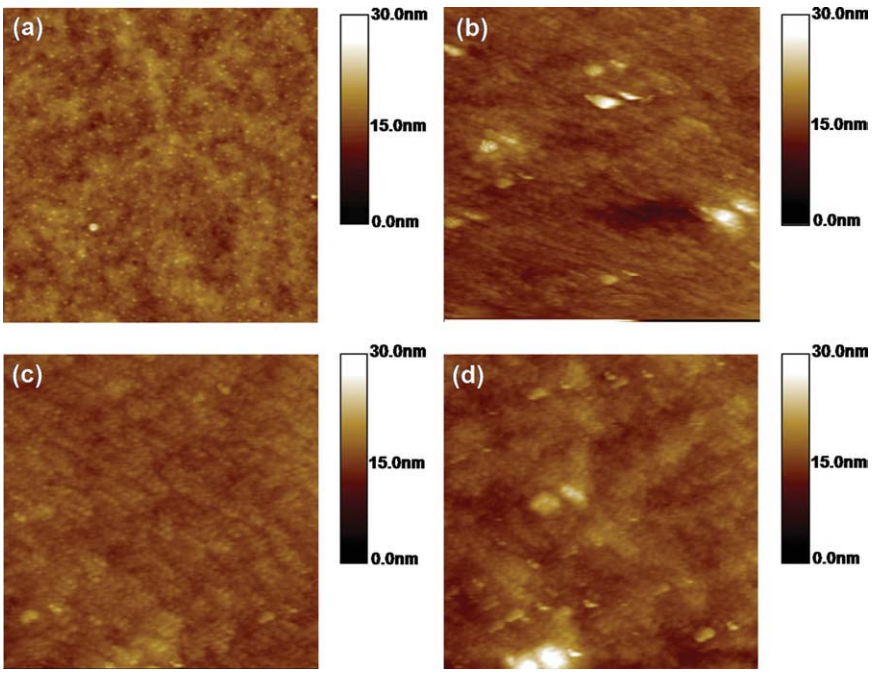

FIGURE 6 Topographic AFM images of films of PCBM blends (1:1, w/w) with (a) the self-made P3HT and (b–d) the copolymers (b) **P05**, (c) **P15**, and (d) **P20**. Image size: 2.5 μm × 2.5 μm.

polymer side chains. We observed PL quenching for the copolymers incorporating pendant electron-deficient 1,3,4-oxadiazole moieties on their side chains. The photocurrents of devices were enhanced in the presence of an optimal amount of the 1,3,4-oxadiazole moieties, thereby leading to improved power conversion efficiencies. The photovoltaic device based on the copolymer **P15** and PCBM exhibited a PCE of 2.50% under AM 1.5 illumination (100 mW cm^{-2}). The EQE of the device incorporating this polythiophene presenting side chain–tethered 1,3,4-oxadiazole units was greater than that of the device incorporating low-molecular-weight P3HT; as a result, its short-circuit current density was also much higher.

The authors thank the National Science Council for the financial support (project NSC 97-2120*M*-009-006) and Yao-Te Chang and So-Lin Hsu for assistance with the synthesis of the polymers.

REFERENCES AND NOTES

1 Yu, G.; Gao, J.; Hummelen, J. C.; Wudl, F.; Heeger, A. J. Science 1995, 270, 1789–1791.

2 Marcos Ramos, A.; Rispens, M. T.; Van Duren, J. K. J.; Hummelen, J. C.; Janssen, R. A. J. J Am Chem Soc 2001, 123, 6714–6715.

3 Egbe, D. A. M.; Nguyen, L. H.; Schmidtke, K.; Wild, A.; Sieber, C.; Guenes, S.; Sariciftci, N. S. J Polym Sci Part A: Polym Chem 2007, 45, 1619–1631.

4 Tang, W. H.; Kietzke, T.; Vemulamada, P.; Chen, Z.-K. J Polym Sci Part A: Polym Chem 2007, 45, 5266–5276.

5 Zhang, F.; Perzon, E.; Wang, X. J.; Mammo, W.; Andersson, M. R.; Inganäs, O. Adv Funct Mater 2005, 15, 745–750.

6 Chiu, M. Y.; Jeng, U. S.; Su, C. H.; Liang, K. S.; Wei, K. H. Adv Mater 2008, 20, 2573–2578.

7 Ego, C.; Marsitzky, D.; Becker, S.; Zhang, J.; Grimsdale, A. C.; Müllen, K.; MacKenzie, J. D.; Silva, C.; Friend, R. H. J Am Chem Soc 2003, 125, 437–443.

8 Lee, Y.; Fukukawa, K.-I.; Bang, J.; Hawker, C. J.; Kim, J. K. J Polym Sci Part A: Polym Chem 2008, 46, 8200–8205.

9 He, Y. J.; Wu, W. P.; Liu, Y. Q.; Li, Y. F. J Polym Sci Part A: Polym Chem 2009, 47, 5304–5312.

10 Sivula, K.; Ball, Z. T.; Watanabe, N.; Fréchet, J. M. J. Adv Mater 2006, 18, 206–210.

11 Kim, Y.; Cook, S.; Tuladhar, S. M.; Choulis, S. A.; Nelson, J.; Durrant, J. R.; Bradley, D. D. C.; Giles, M.; McCulloch, I.; Ha, C.-S.; Ree, M. Nat Mater 2006, 5, 197–203.

12 Li, G.; Shrotriya, V.; Huang, J.; Yao, Y.; Moriarty, T.; Emery, K.; Yang, Y. Nat Mater 2005, 4, 864–868.

13 Erb, T.; Zhokhavets, U.; Gobsch, G.; Raleva, S.; Stühn, B.; Schilinsky, P.; Waldauf, C.; Brabec, C. J. Adv Funct Mater 2005, 15, 1193–1196.

14 Dennler, G.; Scharber, M. C.; Brabec, C. J. Adv Mater 2009, 21, 1323–1338.

15 Huo, L. J.; Tan, Z.; Wang, X.; Zhou, Y.; Han, M. F.; Li, Y. F. J Polym Sci Part A: Polym Chem 2008, 46, 4038–4049.

16 Brabec, C. J.; Sariciftci, N. S.; Hummelen, J. C. Adv Funct Mater 2001, 11, 15–26.

17 Bao, Z.; Peng, Z.; Galvin, M. E.; Chandross, E. A. Chem Mater 1998, 10, 1201–1204.

18 Peng, Q.; Xu, J.; Zheng, W. J Polym Sci Part A: Polym Chem 2009, 47, 3399–3408.

19 Lai, M.-H.; Chueh, C.-C.; Chen, W.-C.; Wu, J.-L.; Chen, F.-C. J Polym Sci Part A: Polym Chem 2009, 47, 973–985.

20 Yuan, M.-C.; Su, M.-H.; Chiu, M.-Y.; Wei, K.-H. J Polym Sci Part A: Polym Chem 2010, 48, 1298–1309.

21 Huang, F.; Chen, K.-S.; Yip, H.-L.; Hau, S. K.; Acton, O.; Zhang, Y.; Luo, J. D.; Jen, A. K.-Y. J Am Chem Soc 2009, 131, 13886–13887.

22 Zhang, S.; Guo, Y.; Fan, H.; Liu, Y.; Chen, H.-Y.; Yang, G.; Zhan, X.; Liu, Y.; Li, Y. F.; Yang, Y. J Polym Sci Part A: Polym Chem 2009, 47, 5498–5508.

23 Chang, Y.-T.; Hsu, S.-L.; Su, M.-H.; Wei, K.-H. Adv Funct Mater 2007, 17, 3326–3331.

24 Chang, Y.-T.; Hsu, S.-L.; Chen, G.-Y.; Su, M.-H.; Singh, T. A.; Diau, E. W.-G.; Wei, K.-H. Adv Funct Mater 2008, 18, 2356–2365.

25 Chang, Y.-T.; Hsu, S.-L.; Su, M.-H.; Wei, K.-H. Adv Mater 2009, 21, 2093–2097.

26 Kim, S.-C.; Park, S.-M.; Park, J. S.; Lee, S.-J.; Jin, S.-H.; Gal, Y.-S.; Lee, J. W. J Polym Sci Part A: Polym Chem 2008, 46, 1098–1110.

27 Chen, Z.-K.; Meng, H.; Lai, Y.-H.; Huang, W. Macromolecules 1999, 32, 4351–4358.

28 Mikroyannidis, J. A.; Spiliopoulos, I. K.; Kasimis, T. S.; Kulkarni, A. P.; Jenekhe, S. A. J Polym Sci Part A: Polym Chem 2004, 42, 2112–2123.

29 Jin, S. H.; Kim, M. Y.; Kim, J. Y.; Lee, K.; Gal, Y. S. J Am Chem Soc 2004, 126, 2474–2480.

30 Rev Schultz, B.; Bruma, M.; Brehmer, L. Adv Mater 1997, 9, 601–613.

31 Zhang, Y.; Huang, F.; Chi, Y.; Jen, A. K.-Y. Adv Mater 2008, 20, 1565–1570.

32 Wang, P.; Chai, C. P.; Wang, F. Z.; Chuai, Y. T.; Chen, X. F.; Fan, X. H.; Zou, D. C.; Zou, Q. F. J Polym Sci Part A: Polym Chem 2008, 46, 1843–1851.

33 Adachi, C.; Tsutsui, T.; Saito, S. Appl Phys Lett 1989, 55, 1489–1491.

34 Lee, K.; Kim, H.-J.; Cho, J. C.; Kim, J. S. Macromolecules 2007, 40, 6457–6463.

35 Huang, S. P.; Liao, J. L.; Tseng, H. E.; Jen, T. H.; Liou, J. Y.; Chen, S. A. Synth Met 2006, 156, 949–953.

36 Wen, S. P.; Pei, J. N.; Zhou, Y. H.; Xue, L. L.; Xu, B.; Li, Y. W.; Tian, W. J. J Polym Sci Part A: Polym Chem 2009, 47, 1003–1012.

37 McCullough, R. D.; Lowe, R. D.; Jayaraman, M.; Anderson, D. L. J Org Chem 1993, 58, 904–912.

38 Iovu, M. C.; Sheina, E. E.; Gil, R. R.; McCullough, R. D. Macromolecules 2005, 38, 8649–8656.

39 Sheina, E. E.; Khersonsky, S. M.; Jones, E. G.; McCullough, R. D. Chem Mater 2005, 17, 3317–3319.

40 Xie, L.-H.; Fu, T.; Hou, X.-Y.; Tang, C.; Hua, Y.-R.; Wang, R.-J.; Fan, Q.-L.; Peng, B.; Wei, W.; Huang, W. Tetrahedron Lett 2006, 47, 6421–6424.

41 Nicolas, M.; Fabre, B.; Marchand, G.; Simonet, J. Eur J Org Chem 2000, 9, 1703–1710.

42 Greczmiel, M.; Strohriegl, P. Macromolecules 1997, 30, 6042–6046.

43 Pommerehne, J.; Vestweber, H.; Guss, W.; Mahrt, R. F.; Bässler, H.; Porsch, M.; Daub, J. Adv Mater 1995, 7, 551–554.

44 Scharber, M. C.; Muhlbacher, D.; Kopper, M.; Denk, P.; Waldauf, C.; Heeger, A. J.; Brabec, C. J. Adv Mater 2006, 18, 789–794.

45 Schilinsky, P.; Asawapirom, U.; Scherf, U.; Biele, M.; Brabec, C. J. Chem Mater 2005, 17, 2175–2180.